Optical properties of fractal aggregates of nanoparticles: Effects of particle size polydispersity

Zahra Naeimi[1] and MirFaez Miri[1,2,*]
[1]*Institute for Advanced Studies in Basic Sciences (IASBS), P.O. Box 45195-1159, Zanjan 45195, Iran*
[2]*Department of Physics, University of Tehran, P.O. Box 14395-547, Tehran, Iran*
(Received 22 July 2009; revised manuscript received 9 November 2009; published 22 December 2009)

We study the effects of particle size dispersion on the absorption spectrum of nonfractal random gas of particles and fractal cluster-cluster aggregates. We use the coupled-dipole equations to describe the interaction of particles with the external electromagnetic wave. We express the absorption in terms of the spectral variable introduced by Bergman [Phys. Rev. B **19**, 2359 (1979)]. In the case of nonfractal clusters, the particle size dispersion has no influence on the overall shape of the spectrum. In the case of fractal clusters, the bandwidth of the spectrum decreases as the particle size dispersion increases. Moreover, the maxima and minima of the spectrum vary, shift, and even disappear, as the particle size dispersion increases.

DOI: 10.1103/PhysRevB.80.224202 PACS number(s): 61.43.Hv, 78.40.Pg, 42.25.Dd

I. INTRODUCTION

Many processes of aggregation of small particles lead to the formation of *fractal* clusters. Fractal carbonaceous soot formed in hydrocarbon fuel burning, metallic (especially silver, gold, or platinum) colloidal clusters, self-affine thin films, and metal-dielectric composites near percolation threshold are a few examples. Due to their fractal structure, these materials exhibit a plethora of intriguing optical properties.[1–4] Inhomogeneous localization of electromagnetic eigenmodes and strong enhancement of local fields,[5] giant enhancement of nonlinear optical responses,[6–9] and femtosecond dynamics of local excitations,[10] have been thoroughly studied. Experiments have proven a 10^6 enhancement of the degenerate four-wave mixing in fractal silver clusters.[6,11] Another fascinating experiment has shown a 10^5 enhancement of two-photon absorption for dyes adsorbed on silver nanoparticle fractal aggregates.[12] It has also been shown than intense laser pulses induce wavelength- and polarization-selective spectral holes in the absorption spectra of fractal aggregates of colloidal particles.[13–15]

In the realm of optics of fractal clusters, the cluster-cluster aggregation (CCA) model[16] has gained much attention.[4,10,17–20] A CCA aggregate consists of N identical polarizable spherical nanoparticles. Most studies are based on the dipole approximation. In this approximation, each sphere of radius R is represented as a point dipole with polarizability $\alpha=R^3(\varepsilon-\varepsilon_h)/(\varepsilon+2\varepsilon_h)$, where ε and ε_h are the dielectric constants of the sphere and host medium, respectively. The local field acting on any dipole is a superposition of the incident field and secondary fields produced by other dipoles. Coupled-dipole equations can be solved to find the dipole moments. Measurable quantities, e.g., the absorption cross-section of the aggregate, can be expressed in terms of the dipole moments. Linear optical properties of *monodisperse* fractal clusters are studied in great detail by Markel *et al.*[17]

There are many good reasons to investigate the effects of particle size *polydispersity* on the optical properties of fractal clusters. (i) Polydisperse fractal clusters are abundant. For example, Xiong and Friedlander[21] found that particles in fractal atmospheric aggregates ranged in size from 6 to 100 nm. (ii) The polarizability of a dielectric sphere of radius R is proportional to R^3. (iii) A system composed of one sphere of radius R_1, and one sphere of radius R_2, is the simplest polydisperse cluster. Even in such a simple system, certain dipole oscillations cannot be excited when $R_1=R_2$.[22] Indeed, the absorption cross-section of dimer can be written as

$$\sigma_a = \tilde{\sigma}_p(R_1^{3/2}+R_2^{3/2})^2k + \tilde{\sigma}_m(R_1^{3/2}-R_2^{3/2})^2k, \qquad (1)$$

where $\lambda=2\pi/k$ is the wavelength of the exciting electromagnetic field. Here the dimensionless factors $\tilde{\sigma}_p$ and $\tilde{\sigma}_m$ depend on the direction of field, the dielectric constants of monomer and host medium, and the distance between two monomers, see Sec. III. In a rough approximation, a cluster can be viewed as an aggregate of dimers. Thus, absorption cross-section of a cluster is expected to be influenced by the particle size polydispersity. (iv) In 1996, Mirkin *et al.*[23] introduced an intriguing DNA-based method for rationally assembling nanoparticles into macroscopic materials. Using 8 and 31 nm gold nanoparticles, they reported preparing materials from building blocks of different sizes.[24] Now it is possible to *tailor* the optical, electronic, and structural properties of the colloidal aggregates by using the specificity of DNA interactions to direct the interactions between particles of different size and composition.[25]

Karpov *et al.*[26] have studied polydisperse aggregates with $N\leq 50$. However, numerical studies[17] indicate that the fractal structure of an aggregate manifests if $N\gtrsim 1000$. Perminov *et al.*[22] introduced an elegant change in variables, which greatly simplifies the coupled-dipole equations for a polydisperse aggregate. They studied *ordered* arrangements of particles: a dimer, a linear aggregate of N particles, a "seven-leafed rosette," etc. In this paper, we study optical properties of bidisperse and polydisperse CCA fractal clusters with $N=1000$ monomers. We find that the particle size dispersion has a deep influence on the bandwidth of the absorption spectrum. The maxima and minima of the spectrum vary, shift, and even disappear, as the particle size dispersion increases.

Our paper is organized as follows. In Sec. II we present coupled-dipole equations for polydisperse clusters. The influence of size dispersion on the optical response of a dimer is discussed in Sec. III. The absorption spectrum of random gas of particles and cluster-cluster aggregates are presented in Sec. IV. Finally, Sec. V contains a summary of our results.

II. COUPLED-DIPOLE EQUATIONS FOR POLYDISPRSE CLUSTERS

We consider the interaction of a plane electromagnetic wave with a polydisperse fractal cluster of N spherical particles. We focus on the quasistatic limit, where the total size of the cluster is much less than the light wavelength λ, and the external electric field $\boldsymbol{E}_0 \exp(-i\omega t)$ is the same at each monomer. We denote the position, radius, polarizability, and light-induced dipole of the ith monomer by $\boldsymbol{r}_i$, R_i, α_i, and $\boldsymbol{d}_i \exp(-i\omega t)$, respectively. The local field acting on any dipole is a superposition of the incident field and all secondary fields produced by the other dipoles. Thus the coupled-dipole equations (CDEs) for the induced dipoles are

$$\boldsymbol{d}_i = \alpha_i \left[\boldsymbol{E}_0 + \sum_{j=1}^{N} W(\boldsymbol{r}_i - \boldsymbol{r}_j)\boldsymbol{d}_j \right], \tag{2}$$

where the interaction tensor $W(\boldsymbol{r}_i - \boldsymbol{r}_j)$ is

$$W_{\alpha,\beta}(\boldsymbol{r}_i - \boldsymbol{r}_j) = \frac{3(\boldsymbol{r}_i - \boldsymbol{r}_j)_\alpha (\boldsymbol{r}_i - \boldsymbol{r}_j)_\beta}{|\boldsymbol{r}_i - \boldsymbol{r}_j|^5} - \frac{\delta_{\alpha\beta}}{|\boldsymbol{r}_i - \boldsymbol{r}_j|^3} \tag{3}$$

for $i \neq j$, and $W_{\alpha,\beta}(\boldsymbol{r}_i - \boldsymbol{r}_j) = 0$ for $i = j$. Here the Greek subscripts denote the Cartesian components. The polarizability of the ith monomer is given by the Lorentz-Lorenz equation

$$\alpha_i = R_i^3 \frac{\varepsilon(\omega) - \varepsilon_h(\omega)}{\varepsilon(\omega) + 2\varepsilon_h(\omega)}, \tag{4}$$

where $\varepsilon(\omega) = \varepsilon'(\omega) + i\varepsilon''(\omega)$ and ε_h are the bulk dielectric permittivity of the sphere and host medium, respectively. The frequency dependence of CDE enters only through $\alpha_i(\omega)$. For monodisperse clusters with arbitrary form of polarizability, Markel *et al.*[27] emphasized the advantages of expressing the solutions of CDE in terms of X and δ which are defined by $\alpha^{-1} = -X - i\delta$.

Following Perminov *et al.*,[22] we introduce

$$\widetilde{\boldsymbol{d}}_i = \boldsymbol{d}_i R_i^{-3/2},$$

$$\widetilde{\alpha}_i = \alpha_i R_i^{-3},$$

$$\widetilde{X} = X_i R_i^3 = -\mathrm{Re}\left(\frac{\varepsilon(\omega) + 2\varepsilon_h(\omega)}{\varepsilon(\omega) - \varepsilon_h(\omega)} \right),$$

$$\widetilde{\delta} = \delta_i R_i^3 = -\mathrm{Im}\left(\frac{\varepsilon(\omega) + 2\varepsilon_h(\omega)}{\varepsilon(\omega) - \varepsilon_h(\omega)} \right),$$

$$\widetilde{Z} = -\widetilde{X} - i\widetilde{\delta},$$

$$\widetilde{\boldsymbol{r}}_{ij} = (\boldsymbol{r}_i - \boldsymbol{r}_j)/\sqrt{R_i R_j}. \tag{5}$$

$\widetilde{X}$ and $\widetilde{\delta}$ are independent of the radii of spheres. Thus, the absorption cross-section of a polydisperse cluster can be studied as a function of the spectral variable $\widetilde{X}$. $\widetilde{\delta}$ characterizes the dissipation of cluster. Note that $\widetilde{Z}$ is simply related to the Bergman-Milton[28] spectral variable $s = \varepsilon_h/(\varepsilon - \varepsilon_h)$. CDE assumes a simple form in terms of the scaled variables

$$\widetilde{Z}\widetilde{\boldsymbol{d}}_i = R_i^{3/2}\boldsymbol{E}_0 + \sum_{j=1}^{N} W(\widetilde{\boldsymbol{r}}_{ij})\widetilde{\boldsymbol{d}}_j. \tag{6}$$

This is a system of $6N$ linear equations to be solved for $\widetilde{\boldsymbol{d}}_i^{\mathrm{R}} = \mathrm{Re}(\widetilde{\boldsymbol{d}}_i)$ and $\widetilde{\boldsymbol{d}}_i^{\mathrm{I}} = \mathrm{Im}(\widetilde{\boldsymbol{d}}_i)$.

Numerical simulation of CDE for monodisperse fractal clusters show that both scaling theory and mean-field theory fail. This is due to inhomogeneous localization of optical eigenmodes, and associated strong field fluctuations.[1–5,17] Therefore, in our study of polydisperse clusters, we focus on the numerical solution of CDE.

In our first approach, we recast the real and imaginary parts of the coupled-dipole Eq. (6)

$$[\widetilde{W}^2 + 2\widetilde{X}\widetilde{W} + (\widetilde{X}^2 + \widetilde{\delta}^2)I]\widetilde{\boldsymbol{d}}^{\mathrm{I}} = \mathcal{E}_0, \tag{7}$$

$$\widetilde{\boldsymbol{d}}^{\mathrm{R}} = -\widetilde{\delta}^{-1}(\widetilde{W} + \widetilde{X}I)\widetilde{\boldsymbol{d}}^{\mathrm{I}}, \tag{8}$$

where $\widetilde{\boldsymbol{d}}^{\mathrm{R}} = (\widetilde{\boldsymbol{d}}_1^{\mathrm{R}}, \widetilde{\boldsymbol{d}}_2^{\mathrm{R}}, \ldots, \widetilde{\boldsymbol{d}}_N^{\mathrm{R}})^t$, $\widetilde{\boldsymbol{d}}^{\mathrm{I}} = (\widetilde{\boldsymbol{d}}_1^{\mathrm{I}}, \widetilde{\boldsymbol{d}}_2^{\mathrm{I}}, \ldots, \widetilde{\boldsymbol{d}}_N^{\mathrm{I}})^t$, $\mathcal{E}_0 = (\widetilde{\delta}R_1^{3/2}\boldsymbol{E}_0, \widetilde{\delta}R_2^{3/2}\boldsymbol{E}_0, \ldots, \widetilde{\delta}R_N^{3/2}\boldsymbol{E}_0)^t$, I is the unity matrix, and t denotes the transpose of a matrix. We use the conjugate-gradient method[29] to solve the above set of $3N$ linear equations for $\widetilde{\boldsymbol{d}}^{\mathrm{I}}$, and then obtain $\widetilde{\boldsymbol{d}}^{\mathrm{R}}$ by a simple matrix-vector multiplication.

Expressing the coupled-dipole equations in terms of the scaled dipoles allows one to follow the approach of Refs. 17, 22, 30, and 31. The matrix $W(\widetilde{\boldsymbol{r}}_{ij})$ is symmetric and commutes with the matrix $\widetilde{Z}I$. Thus one can solve Eq. (6) via decomposing $\widetilde{\boldsymbol{d}}_i$ over the eigenvectors of $W(\widetilde{\boldsymbol{r}}_{ij})$. We found good agreement between two numerical methods.

Now we extend Ref. 30 and express the absorption cross-section of a polydisperse cluster in terms of the dipole moments: $\sigma_a = (4\pi k/|\boldsymbol{E}_0|^2)\sum_{i=1}^{N} |\boldsymbol{d}_i|^2 \delta_i$. The scaled dipoles can be directly used to access the absorption cross-section

$$\sigma_a = \frac{4\pi k\widetilde{\delta}}{|\boldsymbol{E}_0|^2}\sum_{i=1}^{N} |\widetilde{\boldsymbol{d}}_i|^2 = \frac{4\pi k\widetilde{\delta}}{|\boldsymbol{E}_0|^2}(\widetilde{\boldsymbol{d}}^{\mathrm{R}\,2} + \widetilde{\boldsymbol{d}}^{\mathrm{I}\,2}). \tag{9}$$

The scattering cross-section is zero in the quasistatic limit.

III. DIMER

It is instructive to consider the simplest polydisperse cluster. We assume that a sphere of radius R_1 resides at point $(0,0,0)$, and a sphere of radius R_2 resides at point $(0,0,L)$. Introducing $\widetilde{\boldsymbol{d}}_p = \widetilde{\boldsymbol{d}}_1 + \widetilde{\boldsymbol{d}}_2$, $\widetilde{\boldsymbol{d}}_m = \widetilde{\boldsymbol{d}}_1 - \widetilde{\boldsymbol{d}}_2$, and $\boldsymbol{E}_0 = (E_{0x}, E_{0y}, E_{0z})$, the coupled-dipole equations can be written as

$$\widetilde{Z}\widetilde{\boldsymbol{d}}_p = (R_1^{3/2} + R_2^{3/2})\boldsymbol{E}_0 - \frac{R_1^{3/2}R_2^{3/2}}{L^3}\mathrm{diag}(1,1,-2)\widetilde{\boldsymbol{d}}_p,$$

$$\widetilde{Z}\widetilde{\boldsymbol{d}}_m = (R_1^{3/2} - R_2^{3/2})\boldsymbol{E}_0 + \frac{R_1^{3/2}R_2^{3/2}}{L^3}\mathrm{diag}(1,1,-2)\widetilde{\boldsymbol{d}}_m,$$

which are easily solvable. The absorption cross-section $\sigma_a = 2\pi k\widetilde{\delta}(|\widetilde{\boldsymbol{d}}_p|^2 + |\widetilde{\boldsymbol{d}}_m|^2)/|\boldsymbol{E}_0|^2$ is already presented in Eq. (1). Apparently

$$\tilde{\sigma}_p = \frac{(E_{0x}^2 + E_{0y}^2)}{|\boldsymbol{E}_0|^2} \frac{2\pi\tilde{\delta}}{\left(\tilde{X} - \frac{R_1^{3/2}R_2^{3/2}}{L^3}\right)^2 + \tilde{\delta}^2} + \frac{E_{0z}^2}{|\boldsymbol{E}_0|^2} \frac{2\pi\tilde{\delta}}{\left(\tilde{X} + \frac{2R_1^{3/2}R_2^{3/2}}{L^3}\right)^2 + \tilde{\delta}^2}, \quad (10)$$

$$\tilde{\sigma}_m = \frac{(E_{0x}^2 + E_{0y}^2)}{|\boldsymbol{E}_0|^2} \frac{2\pi\tilde{\delta}}{\left(\tilde{X} + \frac{R_1^{3/2}R_2^{3/2}}{L^3}\right)^2 + \tilde{\delta}^2} + \frac{E_{0z}^2}{|\boldsymbol{E}_0|^2} \frac{2\pi\tilde{\delta}}{\left(\tilde{X} - \frac{2R_1^{3/2}R_2^{3/2}}{L^3}\right)^2 + \tilde{\delta}^2}, \quad (11)$$

determine the frequency dependence of σ_a.

The absorption cross-section gains it maximum at frequencies where $\tilde{X} = \pm R_1^{3/2}R_2^{3/2}/L^3$ or $\pm 2R_1^{3/2}R_2^{3/2}/L^3$. Quite remarkably, the resonances at $\tilde{X} = -R_1^{3/2}R_2^{3/2}/L^3$ and $2R_1^{3/2}R_2^{3/2}/L^3$ are absent in the absorption cross-section $\sigma_a = \tilde{\sigma}_p(R_1^{3/2}+R_2^{3/2})^2 k + \tilde{\sigma}_m(R_1^{3/2}-R_2^{3/2})^2 k$ if $R_1 = R_2$. This manifests the influence of size polydispersity on the optical response.[22]

IV. CLUSTERS WITH 1000 MONOMERS

To compare optical properties of nonfractal and fractal clusters, we produced ten samples of the random gas of particles (RGP), and 20 samples of the CCA. The number of monomers in each sample was $N=1000$. Our CCAs were built on a $440a \times 440a \times 440a$ cubic lattice with periodic boundary conditions. The lattice constant a was chosen as the unit of length. Off-lattice RGP was produced in a sphere with the same volume of CCA. Monomers in RGP and CCA fill the same volume fraction ≈ 0.05.

To investigate the effect of size distribution on the optical response, we first studied bidisperse clusters where N_1 monomers have radius R_1 and polarizability α_1, while $N_2 = N - N_1$ monomers have radius R_2 and polarizability $\alpha_2 = \alpha_1(R_2/R_1)^3$. The absorption cross-section of a bidisperse cluster is measured in units of $4\pi k R_e^3$, where the effective radius R_e is defined as $R_e = (N_1R_1^3/N + N_2R_2^3/N)^{1/3}$. We also studied polydisperse clusters whose monomer radius has a uniform distribution in the interval $[R_{\min}, R_{\max}]$. Here

$$R_e = \left(\int_{R_{\min}}^{R_{\max}} \frac{R^3}{R_{\max} - R_{\min}} dR \right)^{1/3}$$

serves as the effective radius. In this model, the distribution of polarizability in the interval $[\alpha_{\min}, \alpha_{\max}]$ is $f(\alpha) = \alpha^{-2/3}/(3\alpha_{\max}^{1/3} - 3\alpha_{\min}^{1/3})$.

The results of simulations were averaged over three different orientations of the incident field for each cluster, and finally averaged over 10 (20) realizations of the RGP (CCA) clusters. We reproduced the results of Ref. 17 for monodisperse RGP and CCA, which serves as a partial test of our program.

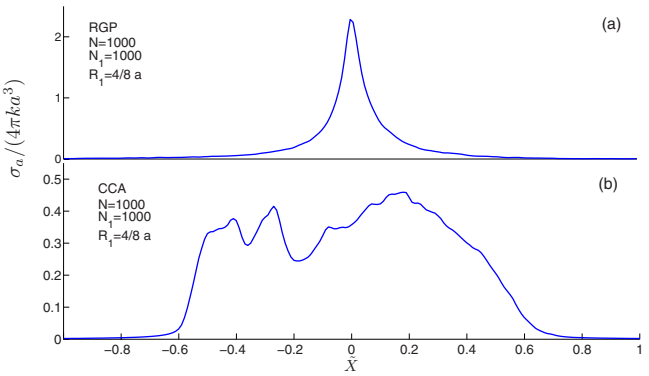

FIG. 1. (Color online) (a) The absorption cross-section σ_a (in units of $4\pi k a^3$) as a function of dimensionless $\tilde{X}$ for monodisperse random gas of particles with $N_1=1000$, $R_1=4a/8$, and $\tilde{\delta}=0.0125$. (b) The absorption cross-section for monodisperse CCA with the same parameters.

A. Random gas of particles

Figure 1(a) delineates σ_a as a function of $\tilde{X}$ for monodisperse random gas of particles with $N_1=1000$, $R_1=4a/8$, and $\tilde{\delta}=0.0125$. The absorption spectrum has *one* clear maximum at $\tilde{X}=0$. Moreover, the spectrum is nearly symmetric. The absorption is considerable in the range $-0.4 < \tilde{X} < 0.4$.

Now we consider a bidisperse RGP with N_1 monomers of radius $R_1=4a/8$, N_2 monomers of radius $R_2=2a/8$, $N=N_1+N_2=1000$ and $\tilde{\delta}=0.0125$. Figure 2 shows σ_a for clusters with $N_2 \in [N/8, 2N/8, 4N/8, 6N/8]$. We find that independently of bidispersity, σ_a is nearly symmetric and gains its maximum at $\tilde{X}=0$. The increase in bidispersity has not a profound effect on the maximum of the normalized absorption cross-section. For $N_2=N/8$ and $6N/8$, the maxima of $\sigma_a/(4\pi k R_e^3)$ are 16.65 and 14.72, respectively.

As another example, we consider a bidisperse RGP with $N_1=N_2=N/2$, $R_1=4a/8$, and $\tilde{\delta}=0.0125$. Figure 3 shows σ_a

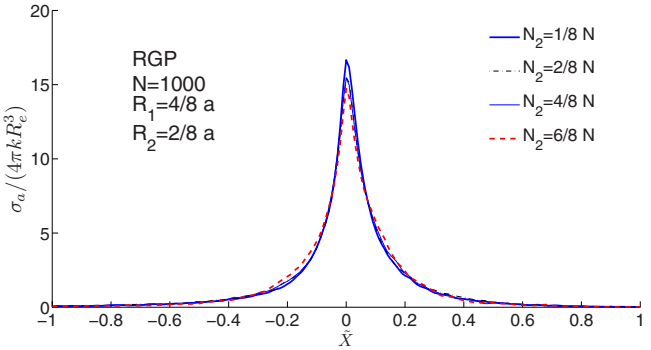

FIG. 2. (Color online) σ_a (in units of $4\pi k R_e^3$) as a function of dimensionless $\tilde{X}$ for bidisperse random gas of particles with N_1 monomers of radius $R_1=4a/8$ and N_2 monomers of radius $R_2=2a/8$. $N=N_1+N_2=1000$ and $\tilde{\delta}=0.0125$.

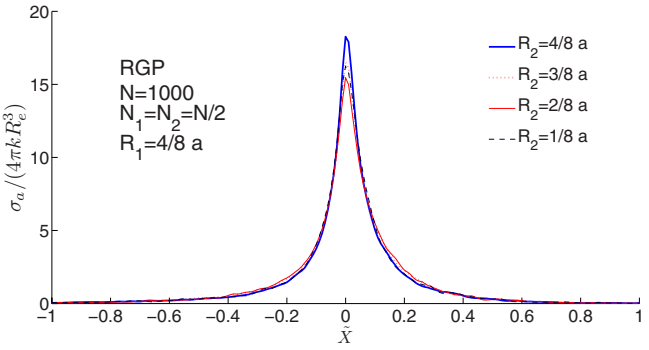

FIG. 3. (Color online) σ_a (in units of $4\pi kR_e^3$) as a function of dimensionless $\tilde{X}$ for bidisperse random gas of particles with $N_1=N_2=N/2$, $R_1=4a/8$, and $\tilde{\delta}=0.0125$.

for various R_2. This figure shows again that independently of bidispersity, σ_a is nearly symmetric and gains its maximum at $\tilde{X}=0$.

To go beyond the bidisperse clusters, we consider a uniform distribution of monomer radius in the interval $[R_{\min},R_{\max}=4a/8]$. Figure 4 shows that the absorption spectrum has one clear maximum at $\tilde{X}=0$.

B. Cluster-cluster aggregates

Figure 1(b) delineates σ_a as a function of $\tilde{X}$ for monodisperse CCA with $N_1=1000$, $R_1=4a/8$, and $\tilde{\delta}=0.0125$. The absorption spectrum has three maxima and two minima which are considerably shifted from $\tilde{X}=0$. There is only one maximum in the $\tilde{X}>0$ region, while there are two maxima and two minima in the $\tilde{X}<0$ region. Apparently σ_a is not an even function of $\tilde{X}$. The absorption is considerable in the range $-0.62<\tilde{X}<0.62$.

Now we consider a bidisperse CCA with N_1 monomers of radius $R_1=4a/8$, N_2 monomers of radius $R_2=2a/8$, $N=N_1+N_2=1000$, and $\tilde{\delta}=0.0125$. Figure 5 shows σ_a for clusters with various N_2. We find that the increase in bidispersity has a clear effect on the maximum of the normalized absorption

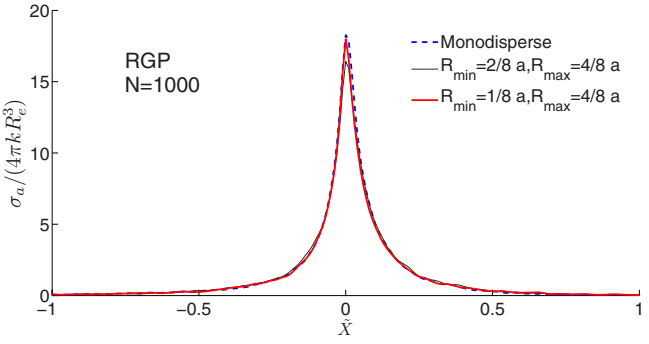

FIG. 4. (Color online) σ_a (in units of $4\pi kR_e^3$) as a function of dimensionless $\tilde{X}$ for polydisperse cluster whose monomer radius has a uniform distribution in the interval $[R_{\min},R_{\max}=4a/8]$. $N=1000$ and $\tilde{\delta}=0.0125$.

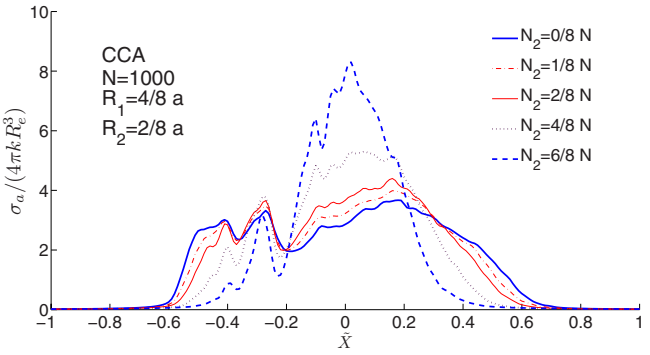

FIG. 5. (Color online) σ_a (in units of $4\pi kR_e^3$) as a function of dimensionless $\tilde{X}$ for bidisperse CCA with N_1 monomers of radius $R_1=4a/8$ and N_2 monomers of radius $R_2=2a/8$. $N=N_1+N_2=1000$ and $\tilde{\delta}=0.0125$.

cross-section. For example, the rightmost peak of $\sigma_a/(4\pi kR_e^3)$ increases from 3.67 to 5.15 as N_2 increases from zero to $4N/8$. Moreover, the absorption bandwidth reduces as bidispersity increases, e.g., the absorption is considerable in the range $-0.48<\tilde{X}<0.45$ when $N_2=6N/8$. A closer inspection reveals that the peak in the $\tilde{X}>0$ region shifts more towards $\tilde{X}=0$ as bidispersity increases. The shift of rightmost peak from $\tilde{X}=0.18$ to 0.02, as N_2 increases from 0 to $6N/8$, is indeed considerable. However, two peaks in the $\tilde{X}<0$ region have no considerable shift.

As another example, we consider a bidisperse CCA with $N_1=7N/8$, $N_2=N/8$, $R_1=4a/8$, and $\tilde{\delta}=0.0125$. Figure 6 shows σ_a for various R_2. As expected, the absorption spectrum of these clusters are not much different from the spectrum of monodisperse cluster. As the population N_2 increases, the spectrum dependence on the radius R_2 becomes clear. Figure 7 shows σ_a for a bidisperse CCA with $N_1=N_2=N/2$, $R_1=4a/8$, and $\tilde{\delta}=0.0125$. We find that the central and rightmost peaks of $\sigma_a/(4\pi kR_e^3)$ increase as R_2 decreases. The rightmost peak shifts towards $\tilde{X}=0$ as R_2 decreases. For example, the right peak shifts from $\tilde{X}=0.18$ to 0.03 as $R_2=4a/8$ decreases to $R_2=a/8$. Here again the absorption bandwidth reduces as bidispersity increases.

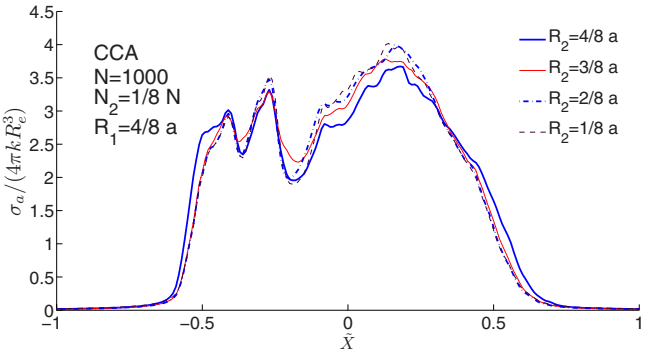

FIG. 6. (Color online) σ_a (in units of $4\pi kR_e^3$) as a function of dimensionless $\tilde{X}$ for bidisperse CCA with $N_1=7N/8$, $N_2=N/8$, $R_1=4a/8$, and $\tilde{\delta}=0.0125$.

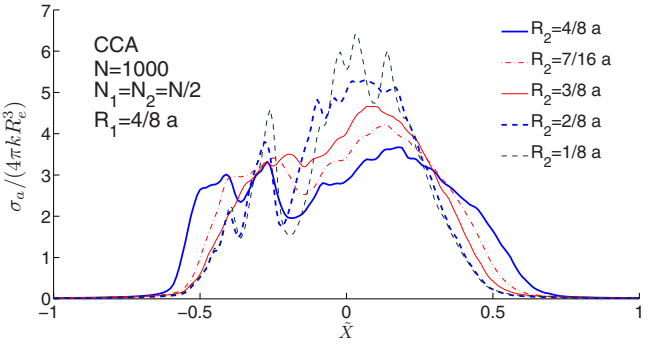

FIG. 7. (Color online) σ_a (in units of $4\pi k R_e^3$) as a function of dimensionless $\tilde{X}$ for bidisperse CCA with $N_1=N_2=N/2$, $R_1=4a/8$, and $\tilde{\delta}=0.0125$.

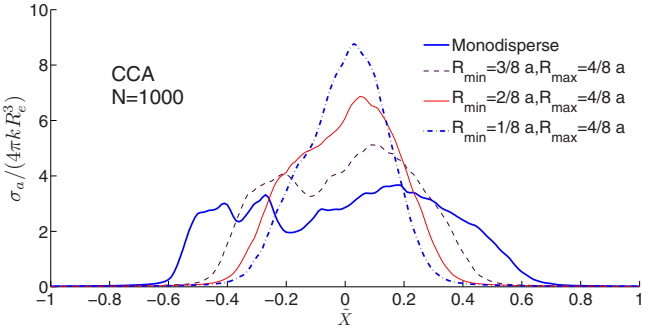

FIG. 8. (Color online) σ_a (in units of $4\pi k R_e^3$) as a function of dimensionless $\tilde{X}$ for polydisperse CCA whose monomer radius has a uniform distribution in the interval $[R_{\min}, R_{\max}=4a/8]$. $N=1000$ and $\tilde{\delta}=0.0125$.

To go beyond the bidisperse CCA, we consider a uniform distribution of monomer radius in the interval $[R_{\min}, R_{\max}=4a/8]$. Figure 8 shows σ_a for various $R_{\min}$. We find that the polydispersity has a deep influence on the absorption spectrum. The absorption spectrum of a monodisperse CCA shows three maxima and two minima. But even for $R_{\min}=3a/8$, the spectrum has two maxima and one minimum. For $R_{\min}=2a/8$ and $a/8$, the spectrum has one maximum and no minimum. The rightmost peak shifts towards $\tilde{X}=0$ as polydispersity increases. The absorption spectrum is not an even function of $\tilde{X}$. The absorption bandwidth reduces as polydispersity increases. Moreover, the peak of $\sigma_a/(4\pi k R_e^3)$ increases as monomer size dispersion grows.

V. SUMMARY

A dimer composed of one sphere of radius R_1 and one sphere of radius R_2, is the simplest polydisperse cluster. Quite remarkably, certain absorption resonances of the dimer disappear as $R_1 \to R_2$. In a rough approximation, a cluster can be viewed as an aggregate of dimers. This immediately suggests that the monomer size dispersion leaves fingerprint on the absorption spectrum of cluster. We prove this point for two important class of clusters: the RGP and the CCA.

The absorption spectra of monodisperse RGP and CCA are obviously different, see Figs. 1(a) and 1(b). The optical properties of fractal aggregates are due to the localization of optical eigenmodes, and associated strong field fluctuations.[1–4] We find that the effects of monomer size (polarizability) dispersion on the spectrum of nonfractal and fractal clusters are quite distinct.

In the case of nonfractal RGP, size dispersion does not change the overall bell shape of the spectrum. Almost independently of the size dispersion, σ_a is nearly symmetric and gains its maximum at $\tilde{X}=0$. The peak of $\sigma_a/(4\pi k R_e^3)$ has a weak dependence on the monomer size dispersion, see Figs. 2–4.

In the case of fractal CCA, the bandwidth of the absorption spectrum clearly decreases as the size dispersion increases. Moreover, the maxima and minima of the spectrum vary, shift, and even disappear, as the size dispersion increases, see Figs. 5–8.

Our work can be extended in many directions: to overcome the limitations of the coupled-dipole equations, one can follow the coupled-multiple method developed in Ref. 19. Nonlinear optical properties of polydisperse fractal aggregates are of immediate interest. We have assumed that all the monomers have the same dielectric constant ε. In a more complicated model, the ith monomer is characterized by its radius R_i and dielectric constant ε_i. For example, consider a fractal aggregate composed of N_1 particles of type 1 (with dielectric constant ε_1 and radius R_1) and let N_2 particles of type 2 (with dielectric constant ε_2 and radius R_2) to attach it. The maxima, minima, and bandwidth of the absorption spectrum depend on N_2. This provides a mechanism for *detecting* particles of importance. This small sensor has potential applications in identification of hazardous molecules, infectious viruses, etc.

*miri@iasbs.ac.ir

[1] *Optics of Nanostructured Materials*, edited by V. A. Markel and T. F. George (Wiley, New York, 2001).

[2] V. M. Shalaev, *Nonlinear Optics of Random Media: Fractal Composites and Metal-Dielectric Films* (Springer-Verlag, Berlin, 2000).

[3] A. K. Sarychev and V. M. Shalaev, Phys. Rep. **335**, 275 (2000).

[4] V. M. Shalaev, Phys. Rep. **272**, 61 (1996).

[5] M. I. Stockman, L. N. Pandey, and T. F. George, Phys. Rev. B **53**, 2183 (1996); M. I. Stockman, Phys. Rev. Lett. **79**, 4562 (1997); Phys. Rev. E **56**, 6494 (1997).

[6] A. V. Butenko, P. A. Chubakov, Y. E. Danilova, S. V. Karpov, A. K. Popov, S. G. Rautian, V. P. Safonov, V. V. Slabko, V. M. Shalaev, and M. I. Stockman, Z. Phys. D: At., Mol. Clusters **17**, 283 (1990).

[7] M. I. Stockman, V. M. Shalaev, M. Moskovits, R. Botet, and T.

F. George, Phys. Rev. B **46**, 2821 (1992).
[8] F. A. Zhuravlev, N. A. Orlova, V. V. Shelkovnikov, A. I. Plekhanov, S. G. Rautian, and V. P. Safonov, JETP Lett. **56**, 260 (1992).
[9] V. M. Shalaev, E. Y. Poliakov, and V. A. Markel, Phys. Rev. B **53**, 2437 (1996).
[10] M. I. Stockman, Phys. Rev. Lett. **84**, 1011 (2000); Phys. Rev. B **62**, 10494 (2000).
[11] S. G. Rautian, V. P. Safonov, P. A. Chubakov, V. M. Shalaev, and M. I. Stockman, Pis'ma Zh. Eksp. Teor. Fiz. **47**, 200 (1988) [JETP Lett. **47**, 243 (1988)].
[12] W. Wenseleers, F. Stellaci, T. Meyer-Friedrichsen, T. Mangel, C. A. Bauer, S. J. K. Pond, S. R. Marder, and J. W. Perry, J. Phys. Chem. B **106**, 6853 (2002).
[13] V. P. Safonov, V. M. Shalaev, V. A. Markel, Yu. E. Danilova, N. N. Lepeshkin, W. Kim, S. G. Rautian, and R. L. Armstrong, Phys. Rev. Lett. **80**, 1102 (1998).
[14] Y. E. Danilova, A. I. Plekhanov, and V. P. Safonov, Physica (Amsterdam) **185A**, 61 (1992).
[15] A. V. Karpov, A. K. Popov, S. G. Rautian, V. P. Safonov, V. V. Slabko, V. M. Shalaev, and M. I. Stockman, JETP Lett. **48**, 571 (1988).
[16] P. Meakin, Phys. Rev. Lett. **51**, 1119 (1983).
[17] V. A. Markel, V. M. Shalaev, E. B. Stechel, W. Kim, and R. L. Armstrong, Phys. Rev. B **53**, 2425 (1996).
[18] V. A. Markel and V. M. Shalaev, J. Opt. Soc. Am. A **18**, 1112 (2001).
[19] V. A. Markel, V. N. Pustovit, S. V. Karpov, A. V. Obuschenko, V. S. Gerasimov, and I. L. Isaev, Phys. Rev. B **70**, 054202 (2004).
[20] S. V. Karpov, V. S. Gerasimov, I. L. Isaev, and V. A. Markel, Phys. Rev. B **72**, 205425 (2005); J. Chem. Phys. **125**, 111101 (2006).
[21] C. Xiong and S. K. Friedlander, Proc. Natl. Acad. Sci. U.S.A. **98**, 11851 (2001).
[22] S. V. Perminov, S. G. Rautian, and V. P. Safonov, J. Exp. Theor. Phys. **98**, 691 (2004).
[23] C. A. Mirkin, R. L. Letsinger, R. C. Mucic, and J. J. Storhoff, Nature (London) **382**, 607 (1996).
[24] R. C. Mucic, J. J. Storhoff, C. A. Mirkin, and R. L. Letsinger, J. Am. Chem. Soc. **120**, 12674 (1998).
[25] J. J. Storhoff and C. A. Mirkin, Chem. Rev. (Washington, D.C.) **99**, 1849 (1999).
[26] S. V. Karpov, A. L. Bas'ko, A. K. Popov, and V. V. Slabko, Colloid J. **62**, 699 (2000).
[27] V. A. Markel, L. S. Muratov, and M. I. Stockman, JETP **71**, 455 (1990).
[28] D. J. Bergman, Phys. Rev. B **19**, 2359 (1979); G. Milton, J. Appl. Phys. **52**, 5286 (1981).
[29] W. H. Press, S. A. Teukolsky, W. T. Vetterling, and B. P. Flannery, *Numerical Recipes in C: The Art of Scientific Computing* (Cambridge University Press, Cambridge, 1999).
[30] V. A. Markel, J. Opt. Soc. Am. B **12**, 1783 (1995).
[31] V. A. Markel, L. S. Muratov, M. I. Stockman, and T. F. George, Phys. Rev. B **43**, 8183 (1991).